ELSEVIER

Polymer 41 (2000) 1345–1353

polymer

Synthesis and characterization of novel segmented polyurethane/clay nanocomposites

T.-K. Chen, Y.-I. Tien, K.-H. Wei*

Department of Materials Science and Engineering, National Chiao Tung University, Hsinchu 30049, Taiwan

Received 25 January 1999; received in revised form 30 March 1999; accepted 7 April 1999

Abstract

A novel segmented polyurethane(PU)/clay nanocomposite has been synthesized by polyurethane and organoclay. 12 aminolauric acid (12COOH) and benzidine (BZD) were used as swelling agents to treat Na^+-montmorillonite and for forming organoclay (12COOH-mont and BZD-mont) through ion exchange. The nanometer-scale silicate layers of organoclay were completely exfoliated in PU in the cases of 1, 3 and 5% 12COOH-mont/PU and in the cases of 1 and 3% BZD-mont/PU nanocomposites as confirmed by X-ray diffraction pattern and transmission electron microscopy studies. The segmented structures of PU were not interfered by the presence of the silicate layers in these nanocomposites as evidenced by their glass transition and degree of phase separation from differential scanning calorimetry and Fourier transform infrared measurements. A two-fold increase in the tensile strength and a three-fold increase in the elongation were found for 1% BZD-mont/PU as compared to that of pure PU. Additionally, both 1% 12COOH-mont/PU and 1% BZD-mont/PU exhibited lower water absorption properties than that of pure PU.

Keywords: Polyurethane; Silicate layers; Nanocomposites

1. Introduction

Polyurethane elastomer is a thermoplastic copolymer with unique properties and can form a variety of starting materials. Hence, this class of materials have received wide attention for their synthesis, morphology, chemical and mechanical properties [1–4]. The linear structure of segmented PU is in the form of $(A–B)_n$. The soft segment part B is normally a polyester or polyether macrogel of molecular weight between 1000 and 3000, and the hard segment part A is composed of a low molecular weight diol or diamine reacted with diisocyanate. Due to the difference in the chemical structure of the soft and the hard segment, phase separation in PU took place easily, and short hard segments formed microdomains by mutual attractions involving intermolecular hydrogen bonding.

Natural clays are composed of oxide layers with cations in between layers. These layered materials are present in the form of the aggregate with a size of about 0.1–10 μm [5,6] consisting of several primary particles with a height of about 8–10 nm. The primary particles are composed of a number of layers, and the thickness of the layers is about 0.96–1.0 nm. In the present investigation, Na^+-montmorillonite was used, and it contained layered silicate structures with the dimensions of $100 \times 100 \times 1\ nm^3$ [5].

Silicate based clay is hydrophilic and lacks affinity with hydrophobic organic polymers. In the coating industry, natural clay has been treated by organic molecules to render it hydrophobic as the organoclay since 1980 [7]. More recently, after the development of Nylon/clay [8–10] nanocomposites by Toyota R&D Labs. in 1990 in Japan, a large number of new composites based on polymer/clay have been investigated, and they are epoxy/clay [11–13], polyimide/clay [14,15], polyethylene oxide/clay [16,17], polycaprolactone/clay [18] and polymethylmethacrylate/clay [19]. In our research laboratory, we have found the accelerated imidization of poly(amic acid) under the presence of clay [20]. Additionally, we developed a two-stage synthesis of polyurethane/clay [21] nanocomposite by first synthesizing polycaprolactone (PCL)/clay nanocomposite and then by replacing a part of 1,4-butanediol (1,4-BG) with the synthesized PCL/clay nanocomposites to form PU/clay nanocomposite. The present study is a continuous effort in developing PU/clay nanocomposite by directly mixing orangoclay with PU. The objectives of this study are to disperse the nanometer-scale silicate layers (12COOH-mont and BZD-mont) to the polyurethane and to investigate their effects on the thermal, mechanical and water absorption properties of PU.

* Corresponding author. Tel.: +886-35-731871; fax: +886-35-724727.

0032-3861/00/$ - see front matter
PII: S0032-3861(99)00280-3

2. Experimental

2.1. Materials

Source clay Swy-2 (Wyoming Na^+-montmorillonite) was obtained from the Clay Minerals Depository at the University of Missouri, Columbus, MO, USA. 12-aminolauric acid (12COOH, TCI), benzidine (BZD, TCI), 4,4′-diphenylmethane diisocyanate (MDI, Aldrich), 1,4-butanediol (1,4-BG, Fisher), polytetramethylene glycol (PTMEG, Mn = 1000, Aldrich) and dimethylformamide (DMF, 99%, Fisher) were used as received.

2.2. Preparation of organoclay

After screening Swy-2 Na^+-montmorillonite with a sieve of 325-mesh to remove impurities, a clay having a cationic exchange capacity of 76.4 meq/l00 g was obtained. 10 g of the screened montmorillonite was gradually added to a prior prepared solution of 12-aminolauric acid (2.16 g) or benzidine (0.89 g), which are dissolved in 1000 ml of 0.01N HCl, at 60°C, and the resultant suspension was vigorously stirred for 3 h. The treated montmorillonite was repeatedly washed by de-ionized water. The filtrate was titrated with 0.1 N $AgNO_3$ until no precipitate of AgCl was formed to ensure the complete removal of chloride ions. The filter cake was then placed in a vacuum oven at 80°C for 12 h for drying. The dried cake was ground and screened with a 325-mesh sieve to obtain the organoclay.

2.3. Synthesis of PU/clay nanocomposite

2.3.1. Preparation of pure polyurethane

Six grams of 4,4-diphenylmethane diisocyanate (MDI) and 12 g of polytetramethylene glycol (PTMEG) at a molar ratio of 2:1 were dissolved in DMF solvent, then the whole solution was heated to 90°C for 2.5 h to form a pre-polymer. Then 1.08 g of 1,4-BG was added to the pre-polymer with rapid stirring at 90°C for 10 min followed by more stirring at room temperature for 3 h to complete the reaction. The final concentration of PU in DMF was 30% by weight. The PU films were formed by casting the solution in a mold and then removing the solvent at 70°C.

2.3.2. Preparation of polyurethane/clay nanocomposite

Different amounts of organoclay (1, 3, 5 wt.%) was mixed with 10 ml of DMF. Following the procedure of synthesizing PU prepolymer as in the previous section and after adding 1,4-BG to the prepolymer at 90°C, the whole PU solution was cooled to room temperature. At room temperature, the solution of organoclay was added to the polyurethane in DMF with stirring for 3 h. After degassing of the mixture and the removal of solvent at 80°C, an elastic film was obtained.

2.3.3. Polymer recovery for molecular weight determination

The synthesized polyurethane/clay (0.2 g) was added to 2 ml of toluene with stirring for 2 h at room temperature. After filtration, a clear polyurethane/clay solution was obtained. The clear polyurethane solution was then gradually dropped under stirring to 4 ml of 1% LiCl/DMF solution. The finished mixture was placed in room temperature for 48 h for performing the reverse ion exchange reaction [22]. After the ion exchange, the solution was centrifuged at 5000 rpm for 5 min. The supernatant liquid was distilled under reduced pressure to remove the solvent, and the pure polyurethane was obtained by reversed ion exchange on the silicate layer.

2.3.4. Characterization

PU/clay samples were scanned at a rate of 4°/min by Mac Science M18 X-ray diffractometer (50 kV, 250 mA) with copper target and Ni-filter. For each interval of 0.01°, the diffracted X-ray intensity was recorded automatically. The differential scanning calorimetry (DSC) and thermogravimetric analyses (TGA) of samples were carried out under N_2 atmosphere with model DSC 2910 and TGA 2950 by Du Pont at a heating rate of 20°C /min. The GPC measurements were performed on pure PU and PU recovered from PU/clay nanocomposites using ion exchange reaction. The molecular weights of the recovered and pure PU were determined by Waters 510 GPC with DMF as the solvent. The calibration curves for GPC were obtained by using polystyrene and polyethylene glycol standards.

Infrared spectroscopic experiments on PU/clay nanocomposites were performed with a Nicolet Ominc 3 Fourier transform infrared spectrometer. 1% solution of the segmented PU and PU nanocomposites in DMF were prepared and coated on KBr disks. In order to remove the residual DMF solvent, the disks were placed in a vacuum oven at 70°C for 24 h. The tensile strength tests were carried out with Instron 4468 machine according to the specifications of ASTM D882. Samples were cut to $100 \times 10 \times 1$ mm^3 in size, and the crosshead speed was set at 500 mm/min. For each data point, five samples were tested, and the average value was taken. The water absorption of segmented PU and PU nanocomposites were carried out according to the specifications of ASTM D570, and the test specimens were cut in the shape of $76.2 \times 25.4 \times 1$ mm^3. The specimens were then placed in a vacuum oven at 80°C for 24 h, and then were cooled in a desiccator, and immediately weighed to the nearest 0.001 g to get the initial weight, W_0. The conditioned specimens were entirely immersed in a container of de-ionized water maintained at 25 ± 0.2°C for 24 h. After 24 h, the specimens were removed from the water, one at a time, surface water on specimens were removed with a dry cloth, and the specimens were weighed immediately to get the final weight, W_1. The percentage of increase in weight of the samples was calculated to the nearest 0.01% by using the formula $(W_1 - W_0)/W_0$. The samples for Transmission Electron Microscopy (TEM) study were first prepared by placing segmented PU/clay into epoxy capsules and the epoxy was cured at 70°C for 24 h in a vacuum oven. Then the cured

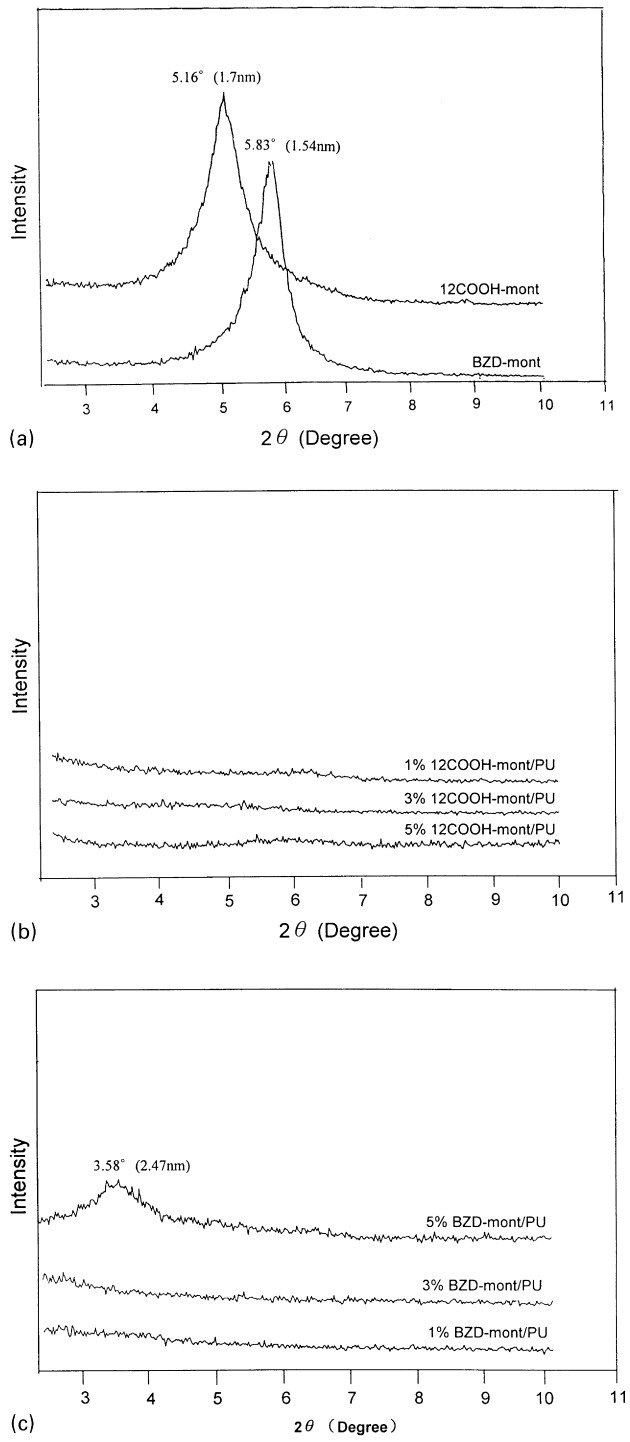

Fig. 1. The X-ray diffraction patterns of: (a) organoclay; (b) different content of 12COOH-mont in PU; and (c) different content of BZD-mont in PU.

epoxies containing PU/clay were microtomed with Leica Ultracut Uct into 80–100 nm thick slices at −80°C. A carbon layer of 3 nm thick was deposited on these slices that being on 200 mesh copper nets for TEM observation. The type of TEM used is JEOL-200FX.

3. Results and discussion

The organoclay modified with 12-aminolauric acid (12COOH) and benzidine (BZD) are termed 12COOH-mont and BZD-mont respectively. The X-ray diffraction (XRD) patterns of 12COOH-mont and BZD-mont are shown in Fig. 1(a). In Fig. 1(a), the d-spacing in 12COOH-mont and BZD-mont are 1.7 and 1.54 nm, respectively, being larger than that of the untreated montmorillonite. The different swollen spacing in these two orangoclay are attributed to the respective size of the swelling agent, with the size of 12-aminolauric acid being larger than that of benzidine.

The XRD patterns of 12COOH-mont/PU and BZD-mont/PU are shown in Fig. 1(b) and (c). In Fig. 1(b), the disappearance of XRD peaks ($2\theta = 2–10°$) in 1, 3 and 5% 12COOH-mont/PU indicated that these silicate layers could be completely exfoliated and dispersed in the PU matrix, being a nanometer-scale composite. For 1 and 3% BZD-mont/PU, exfoliated nanocomposites could also be obtained, as shown in Fig. 1(c). Further evidence of nanometer-scale dispersion of silicate layers in the case of 12COOH-mont/PU and BZD-mont/PU is supported by TEM micrographs, as shown in Fig. 2. In Fig. 2(a) and (b), the TEM photographs of the cross section views of 3% 12COOH-mont/PU and 3% BZD-mont/PU are presented. The thickness of silicate layers of organoclay (darker line) was about 1 nm. The silicate layers were parallel to the surface of the films, and were dispersed in PU. The distance between the silicate layers of organoclay in PU ranged from 4 to 10 nm, which are far larger than the original silicate layers distance of 1.5 nm. This is an evidence that these organoclays are exfoliated in PU. However, for 5% BZD-mont/PU, the formation of nanocomposite was in the form of intercalated structure with d-spacing of 2.47 nm. This can be explained by the fact that the layer distance of BZD-mont is not as large as that of 12COOH-mont (1.54 vs. 1.7 nm). At a higher content of organoclay, a complete and effective entry of PU molecules into the organic modified silicate layers to cause a thorough exfoliation of silicate layers in PU could not be achieved. Additionally, both the end groups of benzidine are amine ($-NH_2$) groups, and they became $-NH_3^+$ ions after HCl treatment. These $-NH_3^+$ ions replaced the Na^+ ions in between the silicate layers and blocked the entry of organic polymer molecules into the silicate layers to further enlarge the molecular spacing thereafter.

The microdomain structures of the segmented PU and the PU/clay were analyzed by FTIR as shown in Figs. 3 and 4. It was found that the positions of peaks for distinctive functional groups were identical both in pure PU and in PU/organoclay, which means that the segmented structure of PU had not been affected by the presence of organoclay, which implied that either the organic modified silicate layers did not react with the PU molecules or reactions

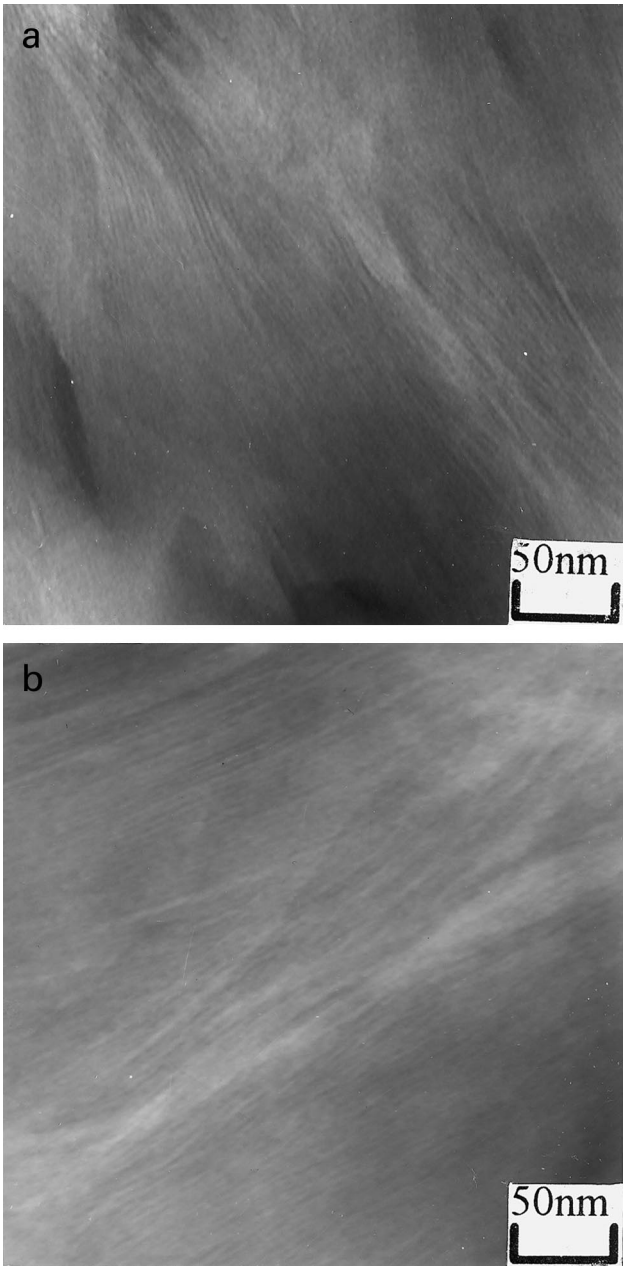

Fig. 2. Transmission electron micrographs of the cross section views of (a) 3% 12COOH-mont/PU, (b) 3% BZD-mont/PU.

between organic modified silicate layers, thus indicating that PU did not cause any detectable change by FTIR.

More specifically, the degree of phase separation in segmented PU can be estimated following the work by Seymour et al. [23]. The 3320 cm^{-1} peak and the 3480 cm^{-1} peak in the IR spectra of pure PU are due to >NH in hydrogen bonding and free >NH groups respectively. In Figs. 3 and 4, all >NH groups of pure PU, 12COOH-mont/PU and BZD-mont/PU participated in hydrogen bonding. The hydrogen bonding was constituted by the >NH groups being as proton donor and the oxygen in carbonyls of the hard segment and in ethers of the soft segment as proton acceptors [23–25]. The formation of hydrogen bonding by –C=O group can be determined by examining the peak position at 1709 cm^{-1} for hydrogen bonded –C=O and at 1731 cm^{-1} for free –C=O. By measuring the peak intensity ratio of these two carbonyl groups, it is possible to give an estimate of the degree of hydrogen bonding. The hydrogen bonding index, R can be defined as the ratio of absorption peak A_{1709}/A_{1731}. In association with the change of absorption peaks of >NH groups, the degree of phase separation and the degree of phase mixing of segmented PU can be calculated [23]. In addition, the hydrogen bonding index, R can be obtained from a baseline approach method:

$$R = C_{\text{bonded}}\varepsilon_{\text{bonded}}/C_{\text{free}}\varepsilon_{\text{free}} = A_{1709}/A_{1731} \quad (1)$$

where C is the concentration and ε is the respective extinction coefficient of bonded and free carbonyl groups. From $\varepsilon_{\text{bonded}}$ and $\varepsilon_{\text{free}}$, it is possible to obtain the degree of participation of –C=O groups in hydrogen bonding. The degree of phase separation (DPS) and degree of phase mixing (DPM) can be obtained by using Eqs. (2) and (3). The ratio of $\varepsilon_{\text{bonded}}/\varepsilon_{\text{free}}$ is taken as 1 according to Cooper [23]:

$$\text{DPS} = C_{\text{bonded}}/(C_{\text{bonded}} + C_{\text{free}}) \quad (2)$$

$$\text{DPM} = 1 - \text{DPS}. \quad (3)$$

Based on these calculations, the DPS and DPM values of organoclay/PU nanocomposites are given in Table 1. As indicated in Table 1, the phase separation ratio in pure PU is about 47%. There was almost no change in DPS and DPM of all 12COOH-mont/PU and BZD-mont/PU nanocomposites, indicating no dependence on the amount of added organoclay. This can be explained by an uniform dispersion of exfoliated silicate layers of organoclay in the nanometer-scale in PU matrix, which cannot be matched by the classical composite materials.

The thermal properties of pure PU, 12COOH-mont/PU, BZD-mont/PU nanocomposites were studied by DSC, and their results are shown in Fig. 5. In Fig. 5, the glass transition temperature of organoclay/PU nanocomposites was between −58 and −59°C, being nearly identical to that of pure PU at −58°C. The effect of small amounts of dispersed silicate layers on the free volume of PU is insignificant to influence the glass transition temperature of pure PU.

The TGA analysis of 12COOH-mont/PU is shown in Fig. 6. In Fig. 6, in the temperature range from 275 to 325°C, the PU/clay nanocomposites contain swelling agent (12COOH) degrades slightly faster than pure PU. This is because the amount of 12COOH used increased with the amount of organoclay in PU. These small organic molecules tend to degrade before the PU polymer, causing a slight weight loss in the nanocomposites. The amount of organic swelling agent in 3 and 5% 12COOH-mont/PU (21 and 35 ppm, respectively) was much higher than that in 1% 12COOH-mont/PU (7 ppm). As a result, the thermal resistance of 3 and 5% 12COOH-mont/PU was also lower than that of pure

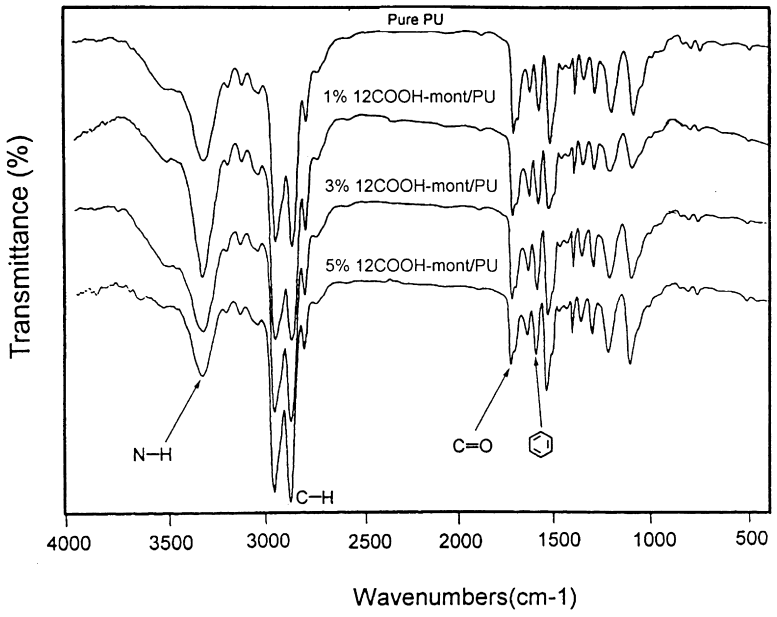

Fig. 3. The FTIR spectra of 12COOH-mont/PU nanocomposites at different content of 12COOH-mont.

PU in the first stage. After a complete decomposition of the swelling agent, the PU/clay nanocomposite displayed higher thermal resistance than that of PU in the temperature range above 400°C because of the presence of clay. For the BZD-mont/PU nanocomposite system, the TGA curves behaved slightly different, as shown in Fig. 7. Both the two terminal $-NH_2$ groups in BZD can replace Na^+ ion to swell the silicate layers. Thus, the amounts of swelling agent for 1, 3, and 5% BZD-mont/PU were 5, 10.5 and 17.5 ppm, respectively, which were just one half of those used in 12COOH-mont/PU composites. This low content and the aromatic nature of BZD provided better thermal resistance than that of 12-aminolauric acid (12COOH) in the nanocomposites. This enabled higher thermal resistance properties of the BZD-mont/PU system at the initial stage of heating. In the later stage of pyrolysis of BZD-mont/PU at 400°C, the overall thermal resistance of BZD-mont/PU nanocomposites was much higher than that of pure PU and 12COOH-mont/PU.

The molecular weight of pure PU and recovered PU from organoclay/PU nanocomposites are given in Table 2. Corresponding to the fact that the segmented PU structures were

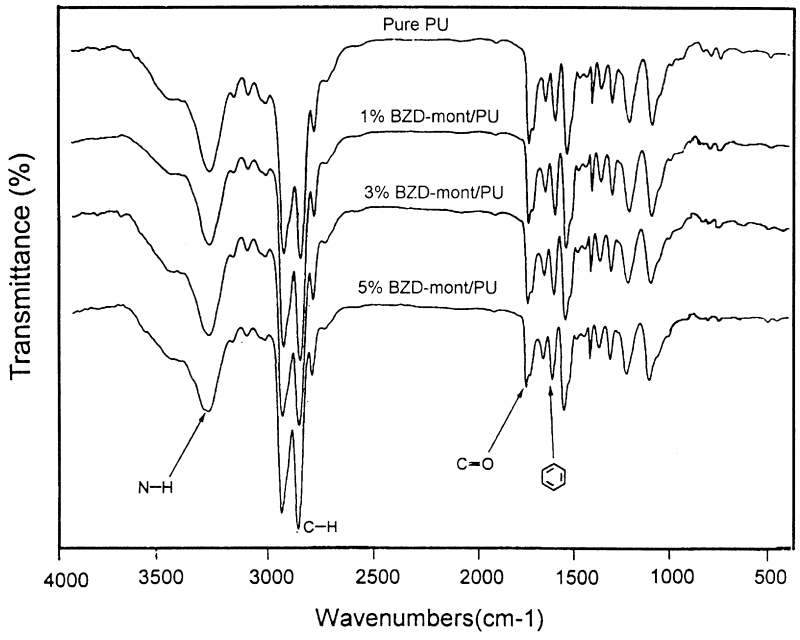

Fig. 4. The FTIR spectra of BZD-mont/PU nanocomposites at different content of BZD-mont.

Table 1
Absorption of carbonyl and degree of phase separation

	$\frac{A_{1709}}{A_{1731}}$	DPM (%)	DPS (%)
Pure PU	0.872	53.4	46.6
1% 12COOH-mont/PU	0.884	53.1	46.9
3% 12COOH-mont/PU	0.876	53.3	46.7
5% 12COOH-mont/PU	0.857	53.8	46.2
1% BZD-mont/PU	0.863	53.7	46.3
3% BZD-mont/PU	0.879	53.2	46.8
5% BZD-mont/PU	0.868	53.5	46.5

not affected by the presence of organoclay as identified by their FTIR spectra, the molecular weight of the recovered PU in general was not strongly affected by the addition of organoclay. Only the molecular weight of PU recovered from BZD-mont/PU showed a slight increase as compared to that of pure PU.

The mechanical properties of organoclay/PU nanocomposites and pure PU are given in Table 2. In Table 2, the tensile strength of 1 and 3% 12COOH-mont/PU is about 16% higher than that of pure PU, and the elongation of 1 and 3% 12COOH-mont/PU is also higher than that of pure PU. However, the tensile strength of 5% 12COOH-mont/PU is lower than that of pure PU, probably because of the high content of 12COOH. In the case of 1% BZD-mont/PU, the tensile strength was twice as that of pure PU, and the elongation is also increased by more than three times of pure PU, indicating a strong effect of BZD-mont on PU. The tensile strength and the elongation of 3 and 5% BZD-mont/PU are

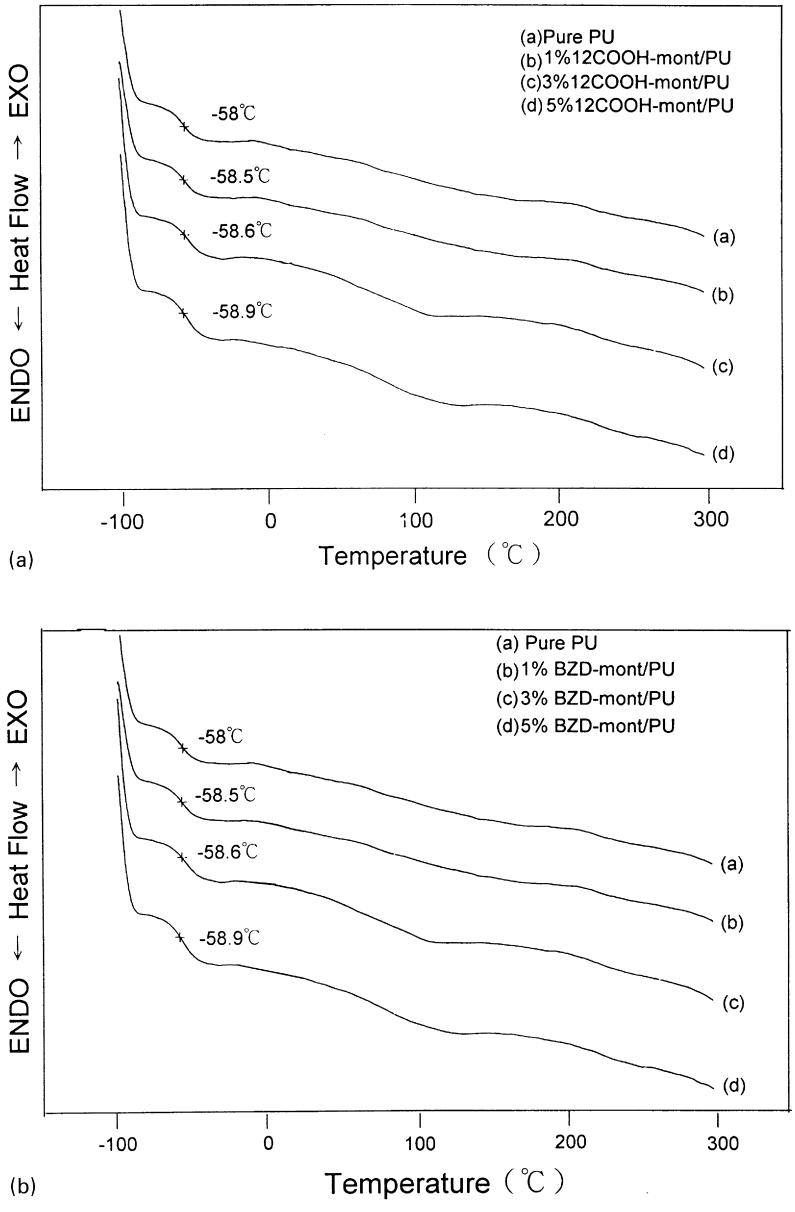

Fig. 5. The d.s.c. curves of (a) pure PU and different content of 12COOH-mont/PU nanocomposites, (b)BZD-mont/PU nanocomposites.

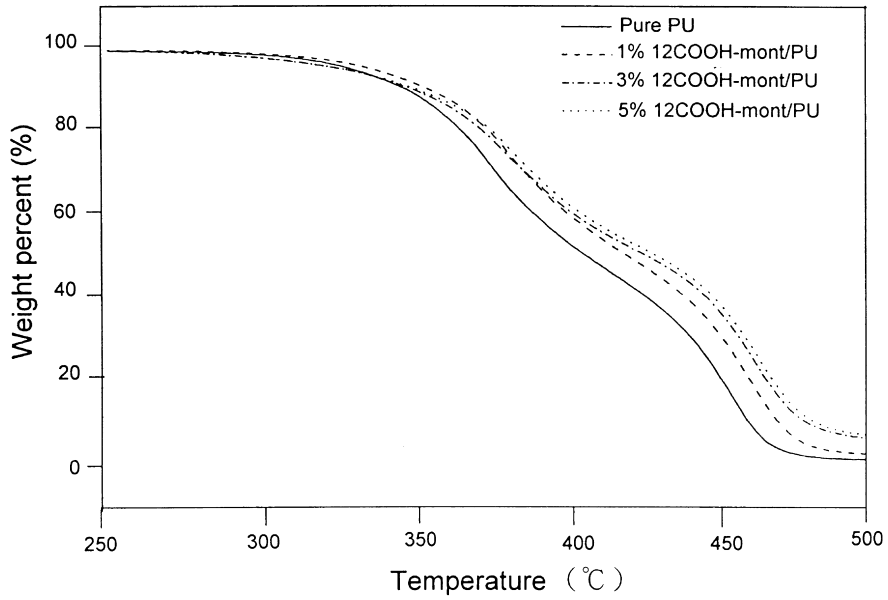

Fig. 6. The t.g.a. curves of 12COOH-mont/PU nanocomposites.

very close to that of 1% BZD-mont/PU. The large contrast between the mechanical behavior of 12COOH mont/PU and BZD-mont/PU can be manifested by the difference in the intermolecular interaction of the swelling agent and the PU molecules. 12COOH contained only one terminal $-NH_2$ group that might react with a minute amount of unreacted –NCO to form urea. BZD had two terminal $-NH_2$ groups that can participate in the reaction with the unreacted –NCO. Therefore, linear branch chains can be formed by 12COOH in PU, and crosslinking can be formed by BZD in PU. The schematic drawing of the intermolecular interaction by 12COOH and BZD in PU is presented in Fig. 8(a) and (b), respectively. During the tensile measurements, the crosslinking by BZD in PU strengthened the intermolecular force between PU molecules, and resulted in much higher tensile strength. The large increase in the elongation of BZD-mont/PU can be attributed to the dispersion of exfoliated silicate layers between the soft and the hard segments and the crosslinking effect.

The water absorption measurements of organoclay/PU nanocomposites were performed according to ASTM D570 and the percentage of water absorption was calculated

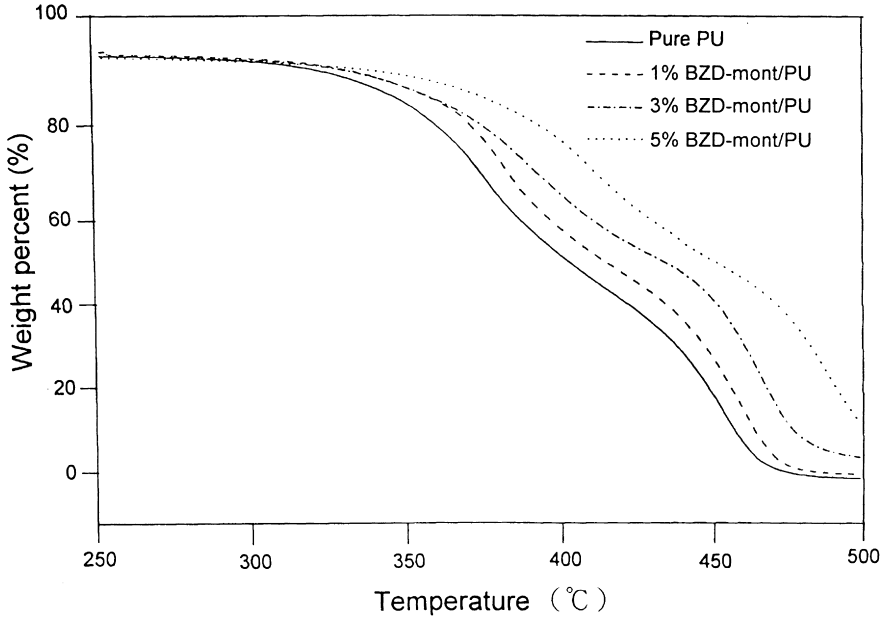

Fig. 7. The t.g.a. curves of BZD-mont/PU nanocomposites.

Table 2
The number-average molecular weight, mechanical properties and water absorption of pure PU and organoclay/PU nanocomposites

	M_n	Tensile strength (kgf/cm^2)	Elongation (%)	Water absorption (%)
Pure PU	10660	66.8	220	1.7
1% 12COOH-mont/PU	11330[a]	76.2	230	1.3
3% 12COOH-mont/PU	10720[a]	76.1	360	1.5
5% 12COOH-mont/PU	10690[a]	53.3	180	1.6
1% BZD-mont/PU	11460[a]	144	680	1.4
3% BZD-mont/PU	11430[a]	130	590	1.6
5% BZD-mont/PU	11040[a]	129	600	1.7

[a] GPC performed on polymer recovered from organoclay/PU nanocomposites using ion exchange reaction.

based on Eq. (4).

$$\text{Water absorption\%} = (W_1 - W_0)\ W_0 \times 100\% \quad (4)$$

where W_1 represents the weight after water absorption and W_0 the dried weight of the sample. The calculated results are given in Table 2. The water absorption ratios of 1, 3 and 5% 12COOH-mont/PU and 1 and 3% BZD-mont/PU were lower than that of pure PU. This phenomenon can be explained by the fact that the mechanism of water absorption of PU/clay was controlled by two competing factors. The first factor is that the clay body itself is water rich, about 8–10%, the water absorption ratio of the nanocomposites will increase with the content of the organoclay. The second factor is that the organoclay layers being dispersed in nanometer-scale in PU matrix can increase the mean free path of water molecules to pass through the network of organoclay/PU than through pure PU [26,27]. These two competitive effects resulted in the lowest water absorption for 1% 12COOH-mont/PU and 1% BZD-mont/PU. When the addition of organoclay became more than 1%, the water absorption function of clay became dominant leading to a slight higher water absorption.

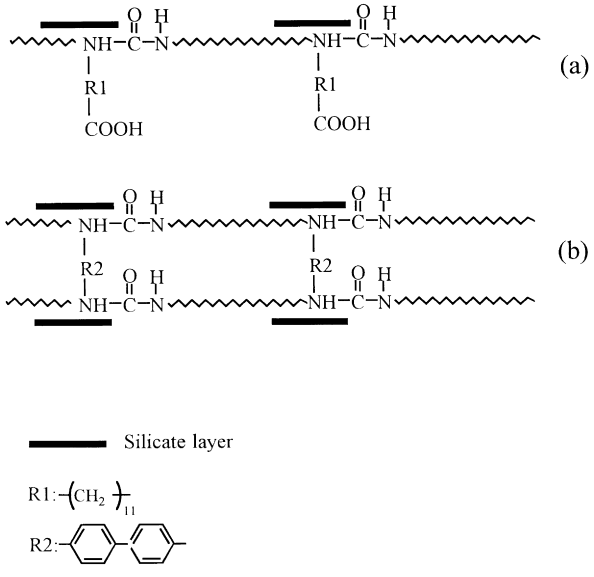

Fig. 8. The schematic drawing of possible intermolecular interaction between PU molecules and (a) 12COOH-mont, (b)BZD-mont.

4. Conclusion

Segmented PU/organoclay nanocomposies have been synthesized with the nanometer-scale silicate layers of organoclay completely exfoliated in PU. The segmented structures of PU were not affected by the presence of the silicate layers in these nanocomposites as evidenced by their glass transition and degree of phase separation. A two-fold increase in the tensile strength and a three-fold increase in the elongation were found for 1% BZD-mont/PU as compared to that of pure PU. Additionally, both 1% 12COOH-mont/PU and 1% BZD-mont/PU exhibited lower water absorption properties than that of pure PU.

Acknowledgements

T.-K. Chen would like to thank the Tze-Chiang Foundation of Science and Technology for providing the time for the research opportunity at the National Chiao Tung University. The financial support provided by National Science Council through project NSC 88-2216-E-009-008 is also appreciated.

References

[1] Penczek P, Frisch KC, Szczepaniak B, Rudnik E. J Polym Sci Polym Chem Ed 1993;31:1211.
[2] Tang W, Farries RJ, Macknight WJ, Eisenbach CD. Macromolecules 1994;27:2814.
[3] Szczepaniak B, Frisch KC, Penczek P, Mejsner J, Leszczynska I, Rudnik E. J Polym Sci Polym Chem Ed 1993;31:3223.
[4] Walkor BM, Rader CP. Handbook of thermoplastic elastomer. New York: Van Nostrand Reinhold, 1988.
[5] Akelah A, Moet A. J Appl Polym Sci: Appl Polym Symp 1994;55:153.
[6] Mahieu-Sicaud A, Mering J, Perrin-Bonnet I. Bull Soc Miner Crystal 1971;74:473.
[7] Calbo LJ. Handbook of coating additives. New York: Marcel Dekker, 1986.
[8] Usuki A. et al. US Pat, 4889885, 1989.

[9] Okada A, Usuki A, Kurauchi T, Kamigaito O. Hybrid organic–inorganic composites. ACS Symposium Series 1995;585:55.
[10] Kojima Y, Usuki A, Kawasumi M, Okada A, Kurauchi T, Kamigaito O. J Polym Sci Part A: Polym Chem 1993;31:1755.
[11] Wang MS, Pinnavaia TJ. Chem Mater 1994;6:468.
[12] Messersmith PB, Giannelis EP. Chem Mater 1994;6:1719.
[13] Lan T, Kaviratna PD, Pinnavaia TJ. Chem Mater 1995;7:2144.
[14] Yano K, Usuki A, Okada A, Kurauchi T, Kamigaito O. J Polym Sci Part A: Polym Chem 1993;31:2493.
[15] Lan T, Kaviratna PD, Pinnavaia TJ. Chem Mater 1994;6:573.
[16] Vaia RA, Vasudevan S, Krawiec W, Scanlon LG, Giannelis EP. Adv Mater 1995;7:154.
[17] Giannelis EP. Adv Mater 1996;8:29.
[18] Messersmith PB, Giannelis EP. J Polym Sci Part A: Polym Chem 1995;33:1047.
[19] Biasci L, Aglietto M, Ruggeri G, Ciardelli F. Polymer 1994;35:3296.
[20] Tyan H-L, Liu Y-C, Wei K-H. Polymer 1999;40:4877.
[21] Chen T-K, Tien Y-I, Wei K-H. J Polym Sci,Part A: Polym Chem 1999;00:000 in press.
[22] Meier LP, Sheldon RA, Caseri WR, Suter UW. Marcomolecules 1994;27:1637.
[23] Seymour RW, Ester GM, Cooper SL. Macromolecules 1970;3:579.
[24] Wang CB, Cooper SL. Macromolecules 1983;16:775.
[25] Lee HS, Wang K, Macknight WJ, Hsu SL. Macromolecules 1988;21:270.
[26] Ward WJ, Gaines GL, Alger MM, Stanley TJ. J Membrane Sci 1991;55:173.
[27] Yano K, et al. J Polym Sci Part A: Polym Chem 1993;31:2493.